Autophagy

Divergent roles of BECN1 in LC3 lipidation and autophagosomal function

Ruina He[a], Jingyu Peng[a], Pengfei Yuan[a], Fang Xu[b] & Wensheng Wei[a]

[a] Biodynamic Optical Imaging Center (BIOPIC); Peking-Tsinghua Center for Life Sciences;
State Key Laboratory of Protein and Plant Gene Research; School of Life Sciences; Peking
University; Beijing, China

[b] State Key Laboratory of Biomembrane and Membrane Biotechnology; Tsinghua University-
Peking University Center for Life Sciences; School of Life Science; Tsinghua University;
Beijing, China
Accepted author version posted online: 08 May 2015.

Click for updates

PLEASE SCROLL DOWN FOR ARTICLE

Divergent roles of BECN1 in LC3 lipidation and autophagosomal function

Ruina He,[1,†] Jingyu Peng,[1,†] Pengfei Yuan,[1] Fang Xu,[2] and Wensheng Wei[1,*]

[1]Biodynamic Optical Imaging Center (BIOPIC); Peking-Tsinghua Center for Life Sciences; State Key Laboratory of Protein and Plant Gene Research; School of Life Sciences; Peking University; Beijing, China; [2]State Key Laboratory of Biomembrane and Membrane Biotechnology; Tsinghua University-Peking University Center for Life Sciences; School of Life Science; Tsinghua University; Beijing, China

[†]These authors contributed equally to this work.

BECN1/Beclin 1 is regarded as a critical component in the class III phosphatidylinositol 3-kinase (PtdIns3K) complex to trigger autophagy in mammalian cells. Despite its significant role in a number of cellular and physiological processes, the exact function of BECN1 in autophagy remains controversial. Here we created a *BECN1* knockout human cell line using the TALEN technique. Surprisingly, the complete loss of BECN1 had little effect on LC3 (MAP1LC3B/LC3B) lipidation, and LC3B puncta resembling autophagosomes by fluorescence microscopy were still evident albeit significantly smaller than those in the wild-type cells. Electron microscopy (EM) analysis revealed that BECN1 deficiency led to malformed autophagosome-like structures containing multiple layers of membranes under amino acid starvation. We further confirmed that the PtdIns3K complex activity and autophagy flux were disrupted in *BECN1*$^{-/-}$ cells. Our results demonstrate the essential role of BECN1 in the functional formation of autophagosomes, but not in LC3B lipidation.

Introduction

Autophagy is responsible for the bulk degradation of cellular organelles and macromolecules to maintain cellular homeostasis.[1,2] During this "self-consuming" process, a closed double-membrane vacuole called autophagosome forms to engulf the unused cellular constituents, and subsequently fuses with the lysosome to form an autolysosome for the degradation.[1-3]

When autophagy is induced, MAP1LC3B/LC3B localizes to the site of autophagosome nucleation and phagophore assembly site from cytoplasm in mammalian cells,[4] and then conjugates to the membrane lipid phosphatidylethanolamine (PE) and becomes membrane-associated to drive vacuolar elongation with other ATG proteins.[5] Thus, the lipidation modification of LC3B from soluble from (LC3B-I) to lipid-modified form (LC3B-II) and its

aggregation in cytoplasm to autophagosomes have been widely used to indicate the occurrence of autophagy.

BECN1, the mammalian ortholog of Vps30/Atg6 in yeast, is evolutionarily conserved and regarded as an essential component for the initiation of conventional autophagy.[6] BECN1 regulates the lipid kinase PIK3C3/VPS34 and forms a stable core of the class III phosphatidylinositol 3-kinase (PtdIns3K) complex with PIK3C3 and PIK3R4/VPS15.[7,8] This complex binds additional proteins such as UVRAG or ATG14 to regulate the autophagy process.[9] ATG14 directs the PtdIns3K (BECN1-PIK3C3/VPS34-PIK3R4/VPS15) complex to form the phagophore assembly site and recruits other ATG proteins for membrane elongation and vesicle completion,[10-13] and the UVRAG-containing complex is involved in both autophagy initiation at early stage and maturation at the late stage.[14,15] Although the suppression of BECN1 impairs the

autophagy-associated post-translational processing of LC3-I to LC3-II,[16-18] BECN1-independent autophagy has been reported, in which LC3B lipidation fails to respond to BECN1 level.[19-33] Notably in yeast cells upon autophagy induction, Atg8 can still be lipidated to form Atg8-PE and exhibit a punctate structure in the absence of Vps30/Atg6, the BECN1 ortholog in yeast.[13,34] It is important therefore to clarify the role of BECN1 in the LC3B lipidation and the overall autophagy function in mammalian cells.

To better understand the role of BECN1 in conventional autophagy pathway in mammalian cells, we created a *BECN1*-knockout HeLa cell line, and investigated the autophagy signaling under usual inducing conditions. To our surprise, BECN1 has little effect on LC3B lipidation, but plays a critical role for the functional formation of autophagosomes and macromolecule degradation through the autophagy pathway.

Results

BECN1 is not required for LC3/LC3B lipidation during autophagy induction

To clarify the role of BECN1 in autophagy, we constructed *BECN1* knockout HeLa cell lines through the TALEN technique

(**Fig. 1A**).[35] Among 45 randomly selected clones that harbor TALEN constructs targeting *BECN1*, BECN1 expression completely disappeared in 11 clones as indicated by immunoblotting analysis (**Fig. 1B**). Sequencing analysis of 6 such clones showed that the loss of BECN1 expression was due to multiple indels occurring at the genome locus of *BECN1*, all of which led to frame shifts and consequently the gene knockout (**Fig. 1C**). To evaluate the basic autophagy pathway in these $BECN1^{-/-}$ clones, we starved these cells by amino acid deprivation and then examined the dynamics of LC3B as indicated by the appearance of the lipidated LC3B (LC3B-II), the phagophore- and autophagosome-specific marker, converted from its unconjugated form (LC3B-I) (**Fig. 1D and Fig. S1**). To our surprise, the LC3B-II/LC3B-I ratio in these $BECN1^{-/-}$ clones in response to the amino acid starvation is comparable to that in the wild-type HeLa cells, while the total LC3B levels in $BECN1^{-/-}$ clones were generally higher than those in the wild type. We then selected one $BECN1^{-/-}$ clone, KO-28, for extensive study, designated as HeLa $BECN1^{-/-}$. The complete loss of BECN1 expression in this very clone was further confirmed by the immunoblotting analysis using 2 antibodies targeting the N- and C-terminal parts of BECN1, respectively (**Fig. 1E**). Since it has been reported that UVRAG stability is dependent on BECN1,[11] we examined the
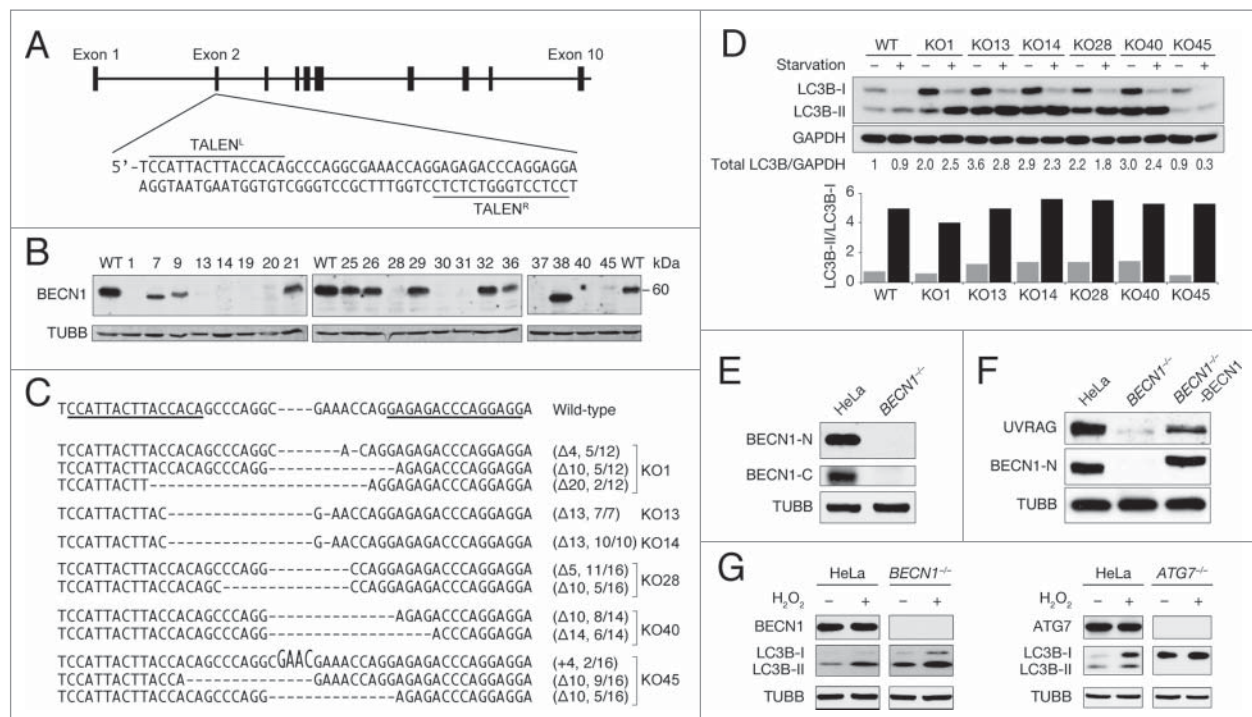
Figure 1. BECN1 is not required for LC3B lipidation during autophagy induction. (**A**) Strategy for knocking out *BECN1* using transcription activator-like effector (TALE) nucleases. Exon 2 was targeted in the locus shown, with the 2 TALE nuclease-binding sequences shown by underlining. (**B**) Immunoblotting analysis of the indicated wild-type cells and different targeted clones for BECN1. The TUBB/β-tubulin bands were used as internal controls in this and other figures. (**C**) Sequence analysis of the *BECN1* gene in the genome of the selected *BECN1* knockout HeLa clones (#1, #13, #14, #28, #40, and #45), the fraction number in the bracket indicates the number of genome PCR clones tested for a particular edition version versus the total PCR clones tested for the single cell clone. (**D**) Immunoblotting analysis of the levels of LC3B-I and LC3B-II of the indicated cells treated with amino acid starvation for 4 h. The GAPDH bands were used as internal protein loading controls in this and other figures. The total LC3B/GAPDH ratio is shown in numbers below each gel lane, and the quantification of relative levels of LC3B-II/LC3B-I is shown in the bar graph. The data were quantified using imageJ in this and other figures. This result was repeated more than 3 times as shown in **Fig. S1**. (**E**) Immunoblotting analysis of the indicated HeLa cell lysates. The monoclonal antibodies targeting N-terminal and C-terminal BECN1 were used. (**F**) Immunoblotting analysis of UVRAG expression in the indicated HeLa cells. (**G**) Immunoblotting analysis of the levels of LC3B-I and LC3B-II of the indicated cells treated by 0.5 mM H_2O_2 for 12 h.

protein level of UVRAG under different conditions, and found that its level was significantly decreased in HeLa $BECN1^{-/-}$, and the exogenous expression of BECN1 was able to restore the level of UVRAG in HeLa $BECN1^{-/-}$ (**Fig. 1F**). Interestingly, the level of BECN1 expression has no effect on BECN1P1/BECN2 expression (**Fig. S2**).[36] These results demonstrate that this isolated clone, HeLa $BECN1^{-/-}$, is a genuine knockout cell line with the complete loss of both BECN1 protein production and its function.

Next, we examined the dynamics of LC3B in HeLa cells with BECN1 knockout or ATG7 knockout when cells were exposed to H_2O_2 (**Fig. 1G**). The absence of BECN1 has little effect on LC3B turnover when autophagy is induced. In contrast, the absence of ATG7 completely blocked LC3B lipidation. These results indicate that, unlike ATG7, BECN1 is not required for the conversion of LC3B-I to LC3B-II during the initiation of autophagy.

BECN1 deficiency results in malformed autophagosomes

To investigate the exact role of BECN1 in autophagy, we examined the morphology of autophagosomes under amino acid starvation. The fluorescence microscopy indicated that amino acid-starved HeLa cells showed an evident increase of the autophagosomes indicated by the green fluorescent LC3B puncta. Similar to those in the wild type, increased amount of LC3B puncta was also observed in HeLa $BECN1^{-/-}$ cells (**Fig. 2A**). The total numbers of LC3B puncta per cell were counted from randomly selected cells under amino acid starvation, and the average numbers of LC3B puncta in wild type were slightly higher than those in BECN1 knockout cells (**Fig. 2B**), suggesting that BECN1 only has marginal effect on the formation of autophagosomes, a result consistent with our above observation (**Fig. 1D**). However, the close-up examination revealed that the sizes of autophagosomes in HeLa $BECN1^{-/-}$ were significantly smaller than those in the wild type (**Fig. 2C**), which was further confirmed by a statistical survey (**Fig. 2D**).

To investigate the potential difference of the autophagosome structure between the wild type and the BECN1-deficient mutant, we examined the subcellular images of cells under electron microscopy (EM). Unlike double-membrane vesicles in the wild-type HeLa cells indicating autophagosomes under amino acid starvation, a large amount of malformed vesicles manifested by multilayers of membranes were observed in $BECN1^{-/-}$ cells, and the exogenous expression of BECN1 was able to reverse this phenotype (**Fig. 2E**). In addition, there were hardly any autolysosomes in $BECN1^{-/-}$ cells compared to the wild-type or HeLa $BECN1^{-/-}$-BECN1 cells. The statistical survey indicated that the amount of the defective vesicles in $BECN1^{-/-}$ cells was significantly higher than that in the wild-type or $BECN1^{-/-}$-BECN1 cells (**Fig. 2F**). These results demonstrate that BECN1 is important for the formation of the normal structure of autophagosomes.

### Autophagy flux is blocked in the absence of BECN1

Although the deficiency of BECN1 has little effect on the LC3B lipidation, the autophagosomes appeared abnormal and much smaller than those in the wild-type cells. To determine whether these malformed multimembrane autophagosome-like structures retain their full function, we monitored the SQSTM1/p62 degradation and LC3B turnover in the presence of a downstream inhibitor under amino acid starvation. The SQSTM1 degradation was observed in both HeLa and HeLa $BECN1^{-/-}$-BECN1, but not in HeLa $BECN1^{-/-}$ cells (**Fig. 3A and B**). Furthermore, using bafilomycin A_1 (BafA1), an inhibitor that blocks the vacuolar-type ATPase and hence autophagosome-lysosome fusion, to monitor autophagy flux, we found that the fold-increase of LC3B-II/LC3B-I was lower in the starved $BECN1^{-/-}$ cells than in the wild-type cells (**Fig. 3C and D and Fig. S3**), suggesting that BECN1 is essential for the overall autophagy flux to degrade the autophagosome-enclosed material, such as long-lived proteins.

BECN1 is required for PtdIns3K activity

Given the fact that BECN1 does not contribute to LC3B lipidation, we wondered whether BECN1 affects the formation of the PtdIns3K complex. The endogenous coimmunoprecipitation (coIP) assay showed that the amount of UVRAG or ATG14 precipitated with PIK3C3 decreased dramatically in HeLa $BECN1^{-/-}$ cells (**Fig. 4A**). Consistent with our previous observation from the whole cell lysate (**Fig. 1F**), the protein levels of ATG14 and UVRAG in BECN1 mutants were much lower than those in the wild type (**Fig. 4A**), also in agreement with the previous report that the stability of ATG14 or UVRAG is dependent on BECN1.[11] To further determine whether BECN1 specifically affects the interaction of PIK3C3 to ATG14 or UVRAG, we overexpressed PIK3C3, ATG14, and UVRAG with different tags, and conducted the coIP analysis. We found that the interaction of PIK3C3-UVRAG as well as PIK3C3-ATG14 was not affected by the absence of BECN1 (**Fig. S4A**), suggesting that BECN1 does not play a role for the direct interaction between PtdIns3K components, and rather suggesting that it is important to maintain the steady state level of UVRAG and ATG14 to ensure the PtdIns3K complex formation. In a parallel experiment, we found that the interaction of BCL2L1/Bcl⁻xL to either UVRAG or ATG14 was significantly decreased in the absence of BECN1 (**Fig. S4B**), suggesting that BCL2L1 interacts with PtdIns3K complex through BECN1, as previously reported.[37,38]

We then investigated whether BECN1 affects PIK3C3 activity by monitoring ZFYVE1/DFCP1 localization, because it was reported that ZFYVE1, a PtdIns3P-binding protein, is recruited to the endoplasmic reticulum (ER) by PIK3C3-produced PtdIns3P to initiate omegasome formation under starvation conditions.[39] Compared with the wild-type cells, ZFYVE1-GFP-localized omegasomes were significantly reduced in HeLa $BECN1^{-/-}$ cells under amino acid starvation, while exogenous DNA-driven expression of BECN1 restored the reduced omegasome formation in HeLa $BECN1^{-/-}$ (**Fig. 4B and C**). These results demonstrated that BECN1 plays an important role in PIK3C3 activity and omegasome formation, also suggesting that the activation of PIK3C3 and omegasome formation are independent of LC3B lipidation, but important for the functional formation of autophagosomes.
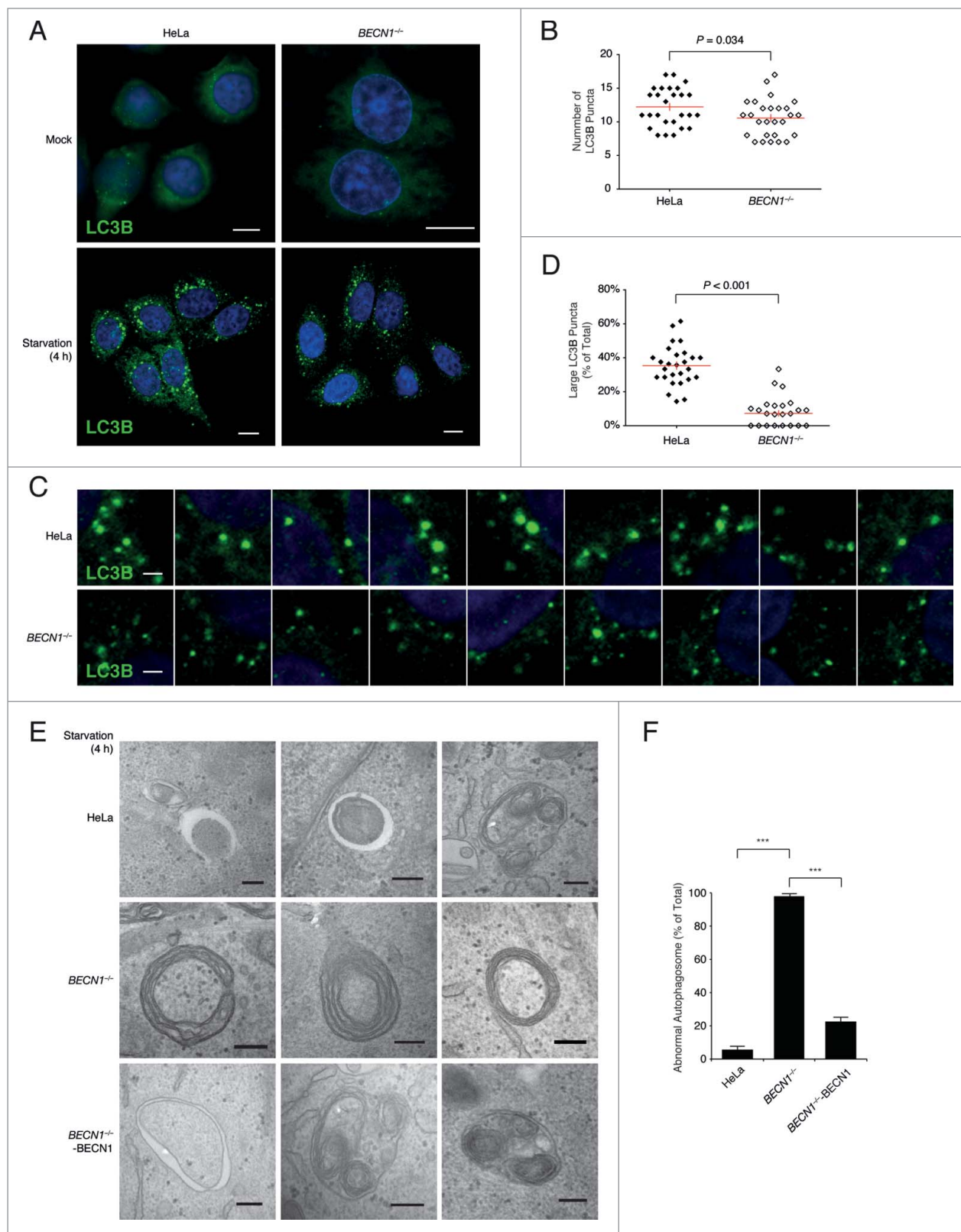
Figure 2. For figure legend, see page 744.

Discussion

Our study, based on the *BECN1* knockout in human cells, clarified the roles of BECN1 in autophagy pathway. First, the complete loss of BECN1 has little effect on LC3B lipidation when autophagy is triggered by starvation or H_2O_2 exposure. Second, the expression of BECN1 is important for the normal structure and function of autophagosomes to ensure autophagy flux.

BECN1 has been regarded as a critical component of PtdIns3K complex to initiate autophagy in mammalian cells.[40,41] LC3B is a protein marker widely used to label autophagosomes since LC3B-II

Figure 3. Effect of BECN1 on autophagy flux. (**A**) Immunoblotting analysis of SQSTM1 degradation and LC3B lipidation in the indicated HeLa cells treated with amino acid starvation for the indicated time. (**B**) The quantification of the immunoblotting results for SQSTM1 degradation from 3 independent experiments. The data indicate the mean ± s.e.m. of SQSTM1/TUBB, n = 3. (**C**) Immunoblotting analysis of LC3B turnover in the indicated HeLa cells treated with amino acid starvation for 4 h in the presence or absence of the autophagy inhibitor bafilomycin A$_1$ (BafA1). (**D**) The bar graph shows the quantification of LC3B-II/LC3B-I ratio of the immunoblotting results from (**C**). These experiments have been repeated 6 times as shown in **Figure S3**.

is reliably associated with phagophores and the completed autophagosomes.[42,43] The effect of BECN1 on LC3B lipidation has been controversial,[16,44,45] our biochemical and fluorescence microscopy data showed that there is little difference in LC3B lipidation between the wild-type and $BECN1^{-/-}$ cells. Similar observations have been reported previously.[44,45]

Further study demonstrated that BECN1 expression is critical for the functional formation of autophagosomes. Although LC3B turnover could be detected in $BECN1^{-/-}$ cells, the autophagosomal structures were aberrant with multiple layers of membranes. These malformed autophagosomes were confirmed to lose their normal function manifested by the degradation of SQSTM1 under autophagy-inducing conditions. In addition, the PtdIns3K complex activity for omegasome formation was suppressed in the absence of BECN1. Therefore, BECN1, just like its ortholog Vps30/Atg6 in yeast, is required for the autophagy pathway in mammalian cells.

Interestingly, the total LC3B background appeared higher in $BECN1^{-/-}$ cells than in the wild type. Since we have observed the increase of both BECN1 and LC3B levels under autophagy-inducing conditions (data not shown), it is unlikely that BECN1 functions as an inhibitor of LC3B production. One plausible explanation is that LC3B, especially its lipidated form LC3B-II that is located on the membrane of autophagosomes and is
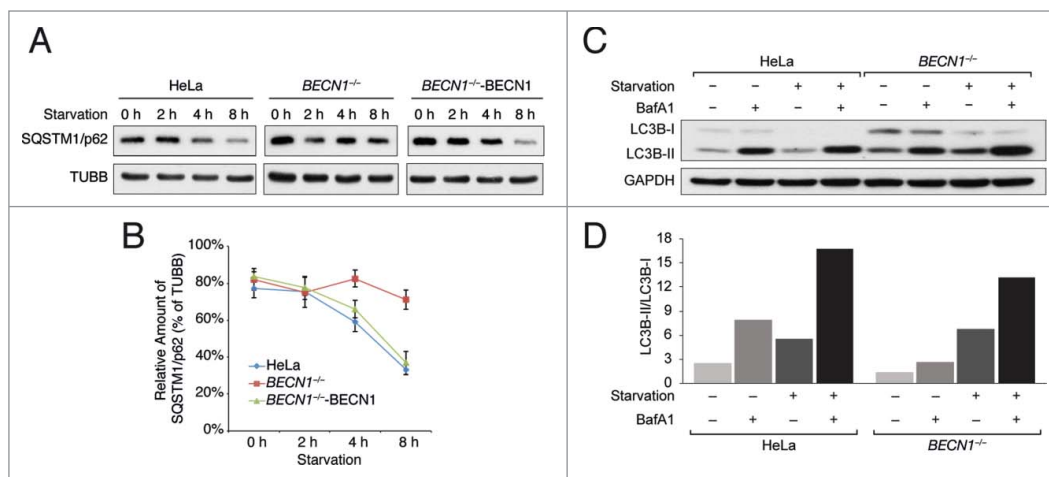
degraded following the maturation of autophagosomes, is readily accumulated in $BECN1^{-/-}$ cells because the malformed autophagosomes lose their capability for macromolecule degradation.

Noticeably, BECN1 is not the only autophagy-essential molecule that has little effect on LC3B turnover. It has been reported that the LC3B-II band is detectable in *rb1cc1/fip200-* and *atg14*-knockout mouse embryonic fibroblasts,[15,46] and in cells with RNA interference-mediated downregulation of ATG13, ATG14, and PIK3C3, where autophagosome formation and autophagic flux are profoundly or completely blocked.[11,16,46,47] Similarly, Atg8 lipidation is unaffected in *atg1, atg2, vps30/atg6, atg9, atg13, atg14, atg16*, and *atg17* mutants in yeast.[13] Taken together, it is noteworthy that these LC3 lipidation-independent autophagy-related proteins are mainly associated with 2 complexes, ULK1-ATG13-RB1CC1 and the PtdIns3K complexes, both involved in the very early stage of autophagy initiation.

Materials and Methods

Cell lines and medium

HeLa cells were cultured in Dulbecco's Modified Eagle's Medium (Gibco 12800-017) containing 10% fetal bovine serum (Hyclone SN30087.02).

Figure 2 (See previous page). Effect of BECN1 on autophagosome formation. (**A**) Autophagosome detection in both wild-type and *BECN1* knockout HeLa cells. Cells were treated with amino acid starvation and analyzed for LC3B-positive autophagosome signals by fluorescence microscopy. DAPI was used to stain nuclear DNA in this and other figures. Scale bar: 10 μm. (**B**) The statistical analysis of the number of autophagosomes in the indicated HeLa cells by Imaris software from (**A**). The data are the mean ± s.e.m., n = 27; the Student *t* test. (**C**) Fluorescence microscopy images of LC3B-positive autophagosomes from the indicated HeLa cells. Nine images from each cell type were randomly selected. Cells were treated the same as in (**A**). Scale bar: 2 μm. (**D**) The statistical analysis of the number of autophagosomes with large size (diameter > 0.5 μm) in the indicated HeLa cells by Imaris software from (**C**). The data are the mean ± s.e.m., n = 27; the Student *t* test. (**E**) The electronic microscopy results for autophagosome detection under amino acid starvation in the indicated HeLa cells. Scale bar: 200 nm. (**F**) The statistical analysis of the percentage of abnormal autophagosomes per 50 total autophagosomes from (**E**). The data are the mean ± s.e.m., n = 3; the Student *t* test; ***P < 0.0001.
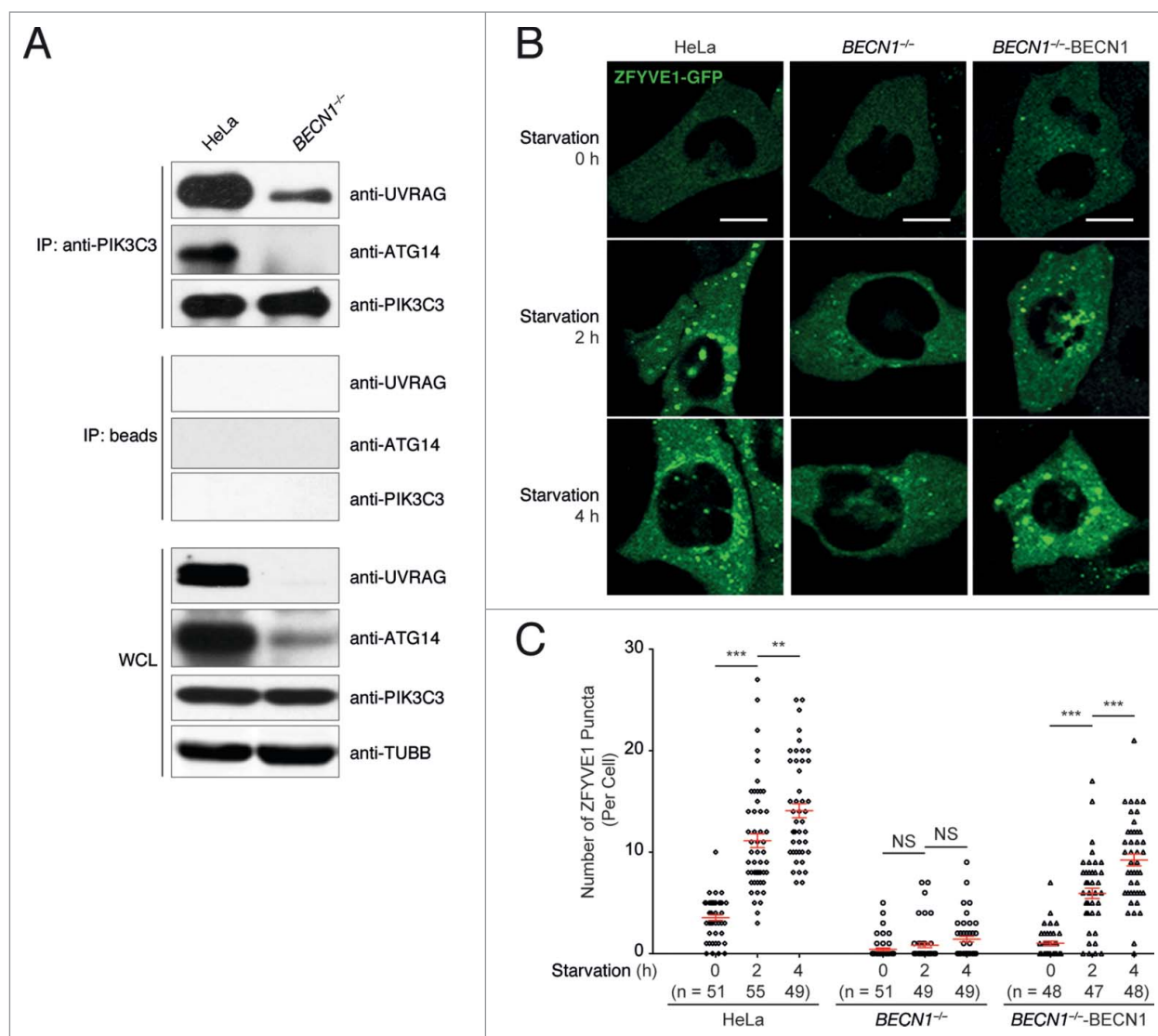
Figure 4. Role of BECN1 on PIK3C3 activity and PtdIns3K complex formation. (**A**) The endogenous protein-protein interaction between PIK3C3 and ATG14 or PIK3C3 and UVRAG in the indicated HeLa cells. Cells were lysed by NP40 lysis buffer. Cell lysates were immunoprecipitated with anti-PIK3C3 antibody or protein A beads only as indicated (WCL, whole cell lysate). (**B**) Detection of omegasomes in the indicated HeLa cells. ZFYVE1-GFP expression plasmid was introduced into cells by electroporation. The fluorescence microscopy images of cells subjected to amino acid starvation for the indicated time were collected using a live-cell imaging system. Scale bar: 10 μm. (**C**) The statistical results of omegasome number in the indicated HeLa cells. The data are the mean $\pm$ s.e.m.; **$P = 0.0032$; ***$P < 0.0001$; NS, not significant; the Student t test.

Antibodies and reagents

Monoclonal antibodies against LC3B (M186-3), ATG7 (PM039) and SQSTM1/p62 (PM045) were from MBL. Monoclonal antibodies targeting N-terminal BECN1 (3495), UVRAG (5320), and MYC-Tag (71D10, rabbit, 2278s) were from Cell Signaling Technology. Anti-C-terminal BECN1 monoclonal antibody (612112) was from BD Transduction Laboratories. Polyclonal antibody against BECN1P1/BECN2 (NB110-60984) was ordered from Novus Biologicals. Flag-HRP monoclonal antibody (A8592) was ordered from Sigma. The secondary antibodies HRP-conjugated goat anti-mouse IgG (H+L) (115-035-003) and HRP-conjugated goat anti-rabbit IgG (H+L) (111-035-003) were purchased from Jackson ImmunoResearch.

The NP40 detergent solution (85124) was purchased from Thermo, and protein A beads (17-0963-02) were from GE Health Care.

Plasmids

The GFP-ZFYVE1 constructs were kindly provided by Li Yu (Tsinghua University). pcDNA4-BECN1-Flag (24388) and pcDNA4-PIK3C3-Flag (24398) were purchased from Addgene. pEF-ATG14 and pEF-UVRAG were constructed in the pEF6-BSD-myc/his-B plasmid (Invitrogen, V962-20). BCL2L1-Flag plasmid was kindly provided by Min Fang (Peking University).

Fluorescence microscopy

HeLa cells were grown on glass cover slips in 6-well plates. After starvation treatment, cells were washed with phosphate-buffered saline (Gibco, 10010023) twice, fixed with pre-cooled methanol for 10 min at $-20\,^{\circ}$C, blocked with 1% BSA (Roche, 735094) for one h at room temperature, and incubated in primary antibody (1:100 diluted in 1% BSA) for 1.5 h followed by secondary antibody for one h, all at room temperature. Finally, The coverslips were mounted onto slides using mounting medium containing DAPI solution (Vector Laboratories, Vectashield, H-1200), and the cells were examined by either LSM 510 laser-scanning confocal microscope (Zeiss, Germany) or a TCS SP2 spectral confocal system (Leica, Germany).

Immunoblotting analysis and coimmunoprecipitation (coIP)

For immunoblotting, cells were treated by H_2O_2 exposure or amino acid starvation (amino acid-free Earle's Balanced Salt Solution, HyClone, SH30029.02) for different time periods, and then lysed for immunoblotting analysis according to standard protocol.[48] For CoIP assay, plasmids were transfected into HeLa cells prior to different treatment and the cells were lysed by NP40 lysis buffer (1% NP40, 150 mM NaCl, 50 mM Tris-Cl, pH 7.4) and subjected for immunoprecipitation analysis according to the manufacturer's protocol of Sigma anti-Flag M2 affinity gel (Sigma, A2220).

Electron microscopy

The cells were fixed using 2.5% glutaraldehyde and 100 mM phosphate buffer, pH 7.2, one to 1.5 h at room temperature. The cells were washed 3 times for 30 min each with 100 mM phosphate buffer, pH 7.2. After the final wash, the cell were post-fixed for 1 h with 1% OsO_4 +1.5% $KFe(CN)_6$. The cells were washed 3 times for 30 min and then dehydrated and embedded in resin (Sigma, SPI-Pon 812). Ultrathin sections (70 nm) were mounted on formvar/carbon coated copper grids and then stained with 2% uranyl and lead citrate and imaged on a transmission electron microscope under 80kV (H-7650B; Hitachi Limited, Japan). Images were acquired using a digital AMT V600 camera (AMT Corp, USA).

Statistical procedures

All data in the images were selected randomly using the Imaris software and presented as mean ± s.e.m., and P values were determined by the Student t test.

Construction of stable knockout cell lines using the TALEN technique

The design and assembly of the 2 pairs of TALENs constructs used for *BECN1* and *ATG7* gene-knockout were based on our own ULtiMATE protocol.[35] More specifically, the 2 targeting sequences for *BECN1* loci are5′-CCATTACTTACCACA-3′ for TALEN^L and 5′-CCTCCTGGGTCTCTC-3'for TALEN^R, with a spacer sequence (5′-gcccaggcgaaaccag-3'); and the 2 targeting sequences for *ATG7* loci are 5′-CCTGGACTCTCTAAA-3′ for TALEN^L and 5′-CCAAGGCACTACTAA-3′ for TALEN^R, with a spacer sequence (5′-ctgcagtttgcccctt-3′). The identification and verification of gene knockout events were based on both sequencing analysis of genome PCR fragments of targeting loci (for *BECN1*) and immunoblotting analysis using antibodies specifically targeting BECN1 or ATG7.

Disclosure of Potential Conflicts of Interest

No potential conflicts of interest were disclosed.

Supplemental Material

Supplemental data for this article can be accessed on the publisher's website.

References

1. Klionsky DJ, Emr SD. Autophagy as a regulated pathway of cellular degradation. Science 2000; 290:1717-21; PMID:11099404; http://dx.doi.org/10.1126/science.290.5497.1717

2. Levine B, Kroemer G. Autophagy in the pathogenesis of disease. Cell 2008; 132:27-42; PMID:18191218; http://dx.doi.org/10.1016/j.cell.2007.12.018

3. Shintani T, Klionsky DJ. Autophagy in health and disease: a double-edged sword. Science 2004; 306:990-5; PMID:15528435; http://dx.doi.org/10.1126/science.1099993

4. Geng J, Klionsky DJ. The Atg8 and Atg12 ubiquitin-like conjugation systems in macroautophagy. 'Protein modifications: beyond the usual suspects' review series. EMBO Rep 2008; 9:859-64; PMID:18704115; http://dx.doi.org/10.1038/embor.2008.163

5. Xie Z, Klionsky DJ. Autophagosome formation: core machinery and adaptations. Nat Cell Biol 2007; 9:1102-9; PMID:17909521; http://dx.doi.org/10.1038/ncb1007-1102

6. Liang XH, Kleeman LK, Jiang HH, Gordon G, Goldman JE, Berry G, Herman B, Levine B. Protection against fatal Sindbis virus encephalitis by beclin, a novel Bcl-2-interacting protein. J Virol 1998; 72:8586-96; PMID:9765397

7. Kihara A, Kabeya Y, Ohsumi Y, Yoshimori T. Beclin-phosphatidylinositol 3-kinase complex functions at the trans-Golgi network. EMBO Rep 2001; 2:330-5; PMID:11306555; http://dx.doi.org/10.1093/embo-reports/kve061

8. Tassa A, Roux MP, Attaix D, Bechet DM. Class III phosphoinositide 3-kinase-Beclin1 complex mediates the amino acid-dependent regulation of autophagy in C2C12 myotubes. Biochem J 2003; 376:577-86; PMID:12967324; http://dx.doi.org/10.1042/BJ20030826

9. Zhong Y, Wang QJ, Li X, Yan Y, Backer JM, Chait BT, Heintz N, Yue Z. Distinct regulation of autophagic activity by Atg14L and Rubicon associated with Beclin 1-phosphatidylinositol-3-kinase complex. Nat Cell Biol 2009; 11:468-76; PMID:19270693; http://dx.doi.org/10.1038/ncb1854

10. Sun Q, Fan W, Chen K, Ding X, Chen S, Zhong Q. Identification of Barkor as a mammalian autophagy-specific factor for Beclin 1 and class III phosphatidylinositol 3-kinase. Proc Natl Acad Sci U S A 2008; 105:19211-6; PMID:19050071; http://dx.doi.org/10.1073/pnas.0810452105

11. Itakura E, Kishi C, Inoue K, Mizushima N. Beclin 1 forms two distinct phosphatidylinositol 3-kinase complexes with mammalian Atg14 and UVRAG. Mol Biol Cell 2008; 19:5360-72; PMID:18843052; http://dx.doi.org/10.1091/mbc.E08-01-0080

12. Suzuki K, Kubota Y, Sekito T, Ohsumi Y. Hierarchy of Atg proteins in pre-autophagosomal structure organization. Genes Cells 2007; 12:209-18; PMID:17295840; http://dx.doi.org/10.1111/j.1365-2443.2007.01050.x

13. Suzuki K, Kirisako T, Kamada Y, Mizushima N, Noda T, Ohsumi Y. The pre-autophagosomal structure organized by concerted functions of APG genes is essential for autophagosome formation. EMBO J 2001; 20:5971-81; PMID:11689437; http://dx.doi.org/10.1093/emboj/20.21.5971

14. Matsunaga K, Noda T, Yoshimori T. Binding Rubicon to cross the Rubicon. Autophagy 2009; 5:876-7; PMID:19550146; http://dx.doi.org/10.4161/auto.9098

15. Matsunaga K, Saitoh T, Tabata K, Omori H, Satoh T, Kurotori N, Maejima I, Shirahama-Noda K, Ichimura T, Isobe T, et al. Two Beclin 1-binding proteins, Atg14L and Rubicon, reciprocally regulate autophagy at different stages. Nat Cell Biol 2009; 11:385-96; PMID:19270696; http://dx.doi.org/10.1038/ncb1846

16. Zeng X, Overmeyer JH, Maltese WA. Functional specificity of the mammalian Beclin-Vps34 PI 3-kinase complex in macroautophagy versus endocytosis and lysosomal enzyme trafficking. J Cell Sci 2006; 119:259-70; PMID:16390869; http://dx.doi.org/10.1242/jcs.02735

17. Wang RC, Wei Y, An Z, Zou Z, Xiao G, Bhagat G, White M, Reichelt J, Levine B. Akt-mediated regulation of autophagy and tumorigenesis through Beclin 1 phosphorylation. Science 2012; 338:956-9; PMID:23112296; http://dx.doi.org/10.1126/science.1225967

18. Wei Y, Zou Z, Becker N, Anderson M, Sumpter R, Xiao G, Kinch L, Koduru P, Christudass CS, Veltri RW, et al. EGFR-mediated Beclin 1 phosphorylation in autophagy suppression, tumor progression, and tumor chemoresistance. Cell 2013; 154:1269-84; PMID:24034250; http://dx.doi.org/10.1016/j.cell.2013.08.015

19. Chu CT, Zhu J, Dagda R. Beclin 1-independent pathway of damage-induced mitophagy and autophagic stress: implications for neurodegeneration and cell death. Autophagy 2007; 3:663-6; PMID:17622797; http://dx.doi.org/10.4161/auto.4625

20. Zhu JH, Horbinski C, Guo F, Watkins S, Uchiyama Y, Chu CT. Regulation of autophagy by extracellular signal-regulated protein kinases during 1-methyl-4-phenylpyridinium-induced cell death. Am J Pathol 2007; 170:75-86; PMID:17200184; http://dx.doi.org/10.2353/ajpath.2007.060524

21. Scarlatti F, Maffei R, Beau I, Ghidoni R, Codogno P. Non-canonical autophagy: an exception or an underestimated form of autophagy? Autophagy 2008; 4:1083-5; PMID:18849663; http://dx.doi.org/10.4161/auto.7068

22. Scarlatti F, Maffei R, Beau I, Codogno P, Ghidoni R. Role of non-canonical Beclin 1-independent autophagy in cell death induced by resveratrol in human breast cancer cells. Cell Death Differ 2008; 15:1318-29; PMID:18421301; http://dx.doi.org/10.1038/cdd.2008.51

23. Tian S, Lin J, Jun Zhou J, Wang X, Li Y, Ren X, Yu W, Zhong W, Xiao J, Sheng F, et al. Beclin 1-independent autophagy induced by a Bcl-XL/Bcl-2 targeting compound, Z18. Autophagy 2010; 6:1032-41; PMID:20818185; http://dx.doi.org/10.4161/auto.6.8.13336

24. Raffoul F, Campla C, Nanjundan M. SnoN/SkiL, a TGFbeta signaling mediator: a participant in autophagy induced by arsenic trioxide. Autophagy 2010; 6:955-7; PMID:20699661; http://dx.doi.org/10.4161/auto.6.7.13041

25. Gao P, Bauvy C, Souquere S, Tonelli G, Liu L, Zhu Y, Qiao Z, Bakula D, Proikas-Cezanne T, Pierron G, et al. The Bcl-2 homology domain 3 mimetic gossypol induces both Beclin 1-dependent and Beclin 1-independent cytoprotective autophagy in cancer cells. J Biol Chem 2010; 285:25570-81; PMID:20529838; http://dx.doi.org/10.1074/jbc.M110.118125

26. Smith DM, Patel S, Raffoul F, Haller E, Mills GB, Nanjundan M. Arsenic trioxide induces a beclin-1-independent autophagic pathway via modulation of SnoN/SkiL expression in ovarian carcinoma cells. Cell Death Differ 2010; 17:1867-81; PMID:20508647; http://dx.doi.org/10.1038/cdd.2010.53

27. Grishchuk Y, Ginet V, Truttmann AC, Clarke PG, Puyal J. Beclin 1-independent autophagy contributes to apoptosis in cortical neurons. Autophagy 2011; 7:1115-31; PMID:21646862; http://dx.doi.org/10.4161/auto.7.10.16608

28. Seo G, Kim SK, Byun YJ, Oh E, Jeong SW, Chae GT, Lee SB. Hydrogen peroxide induces Beclin 1-independent autophagic cell death by suppressing the mTOR pathway via promoting the ubiquitination and degradation of Rheb in GSH-depleted RAW 264.7 cells. Free Radic Res 2011; 45:389-99; PMID:21067284; http://dx.doi.org/10.3109/10715762.2010.535530

29. Arsov I, Adebayo A, Kucerova-Levisohn M, Haye J, Macneil M, Papavasiliou FN, Yue Z, Ortiz BD. A role for autophagic protein beclin 1 early in lymphocyte development. J Immunol 2011; 186:2201-9; PMID:21239722; http://dx.doi.org/10.4049/jimmunol.1002223

30. Zhou C, Zhou J, Sheng F, Zhu H, Deng X, Xia B, Lin J. The heme oxygenase-1 inhibitor ZnPPIX induces non-canonical, Beclin 1-independent, autophagy through p38 MAPK pathway. Acta Biochim Biophys Sin 2012; 44:815-822; PMID:22875631; http://dx.doi.org/10.1093/abbs/gms064

31. Liu C, Yan X, Wang HQ, Gao YY, Liu J, Hu Z, Liu D, Gao J, Lin B. Autophagy-independent enhancing effects of Beclin 1 on cytotoxicity of ovarian cancer cells mediated by proteasome inhibitors. BMC Cancer 2012; 12:622; PMID:23270461; http://dx.doi.org/10.1186/1471-2407-12-622

32. Zhang HY, Du ZX, Meng X, Zong ZH, Wang HQ. Beclin 1 enhances proteasome inhibition-mediated cytotoxicity of thyroid cancer cells in macroautophagy-independent manner. J Clin Endocrinol Metab 2012; 98:E217-E226; PMID:23264393; http://dx.doi.org/10.1210/jc.2012-2679

33. Yan C, Oh JS, Yoo SH, Lee JS, Yoon YG, Oh YJ, Jang MS, Lee SY, Yang J, Lee SH, et al. The targeted inhibition of mitochondrial Hsp90 overcomes the apoptosis resistance conferred by Bcl-2 in Hep3B cells via necroptosis. Toxicol Appl Pharmacol 2013; 266:9-18; PMID:23147571; http://dx.doi.org/10.1016/j.taap.2012.11.001

34. Suzuki K, Noda T, Ohsumi Y. Interrelationships among Atg proteins during autophagy in Saccharomyces cerevisiae. Yeast 2004; 21:1057-65; PMID:15449304; http://dx.doi.org/10.1002/yea.1152

35. Yang J, Yuan P, Wen D, Sheng Y, Zhu S, Yu Y, Gao X, Wei W. ULtiMATE System for Rapid Assembly of Customized TAL Effectors. PLoS One 2013; 8: e75649; PMID:24228087; http://dx.doi.org/10.1371/journal.pone.0075649

36. He C, Wei Y, Sun K, Li B, Dong X, Zou Z, Liu Y, Kinch LN, Khan S, Sinha S, et al. Beclin 2 functions in autophagy, degradation of g protein-coupled receptors, and metabolism. Cell 2013; 154:1085-99; PMID:23954414; http://dx.doi.org/10.1016/j.cell.2013.07.035

37. Sinha S, Levine B. The autophagy effector Beclin 1: a novel BH3-only protein. Oncogene 2008; 27(Suppl 1): S137-48; PMID:19641499; http://dx.doi.org/10.1038/onc.2009.51

38. Liang C, Feng P, Ku B, Dotan I, Canaani D, Oh BH, Jung JU. Autophagic and tumour suppressor activity of a novel Beclin1-binding protein UVRAG. Nat Cell Biol 2006; 8:688-99; PMID:16799551; http://dx.doi.org/10.1038/ncb1426

39. Axe EL, Walker SA, Manifava M, Chandra P, Roderick HL, Habermann A, Griffiths G, Ktistakis NT. Autophagosome formation from membrane compartments enriched in phosphatidylinositol 3-phosphate and dynamically connected to the endoplasmic reticulum. J Cell Biol 2008; 182:685-701; PMID:18725538; http://dx.doi.org/10.1083/jcb.200803137

40. Liang XH, Jackson S, Seaman M, Brown K, Kempkes B, Hibshoosh H, Levine B. Induction of autophagy and inhibition of tumorigenesis by beclin 1. Nature 1999; 402:672-6; PMID:10604474; http://dx.doi.org/10.1038/45257

41. Furuya N, Yu J, Byfield M, Pattingre S, Levine B. The evolutionarily conserved domain of Beclin 1 is required for Vps34 binding, autophagy and tumor suppressor function. Autophagy 2005; 1:46-52; PMID:16874027; http://dx.doi.org/10.4161/auto.1.1.1542

42. Mizushima N, Yoshimori T, Levine B. Methods in mammalian autophagy research. Cell 2010; 140:313-26; PMID:20144757; http://dx.doi.org/10.1016/j.cell.2010.01.028

43. Klionsky DJ, Abeliovich H, Agostinis P, Agrawal DK, Aliev G, Askew DS, Baba M, Baehrecke EH, Bahr BA, Ballabio A, et al. Guidelines for the use and interpretation of assays for monitoring autophagy in higher eukaryotes. Autophagy 2008; 4:151-75; PMID:18188003; http://dx.doi.org/10.4161/auto.5338

44. Matsui Y, Takagi H, Qu X, Abdellatif M, Sakoda H, Asano T, Levine B, Sadoshima J. Distinct roles of autophagy in the heart during ischemia and reperfusion: roles of AMP-activated protein kinase and Beclin 1 in mediating autophagy. Circ Res 2007; 100:914-22; PMID:17332429; http://dx.doi.org/10.1161/01.RES.0000261924.76669.36

45. Fogel AI, Dlouhy BJ, Wang C, Ryu SW, Neutzner A, Hasson SA, Sideris DP, Abeliovich H, Youle RJ. Role of membrane association and Atg14-dependent phosphorylation in beclin-1-mediated autophagy. Mol Cell Biol 2013; 33:3675-88; PMID:23878393; http://dx.doi.org/10.1128/MCB.00079-13

46. Hara T, Takamura A, Kishi C, Iemura S, Natsume T, Guan JL, Mizushima N. FIP200, a ULK-interacting protein, is required for autophagosome formation in mammalian cells. J Cell Biol 2008; 181:497-510; PMID:18443221; http://dx.doi.org/10.1083/jcb.200712064

47. Hosokawa N, Hara T, Kaizuka T, Kishi C, Takamura A, Miura Y, Iemura S, Natsume T, Takehana K, Yamada N, et al. Nutrient-dependent mTORC1 association with the ULK1-Atg13-FIP200 complex required for autophagy. Mol Biol Cell 2009; 20:1981-91; PMID:19211835; http://dx.doi.org/10.1091/mbc.E08-12-1248

48. Harlow E, Lane D. Using Antibodies: A Laboratory Manual. Cold Spring Harbor Lab. NY: Press, Plainview; 1999.

Supplementary Materials

Divergent roles of BECN1 in LC3 lipidation and autophagosomal function

Ruina He, Jingyu Peng, Pengfei Yuan, Fang Xu and Wensheng Wei

Biodynamic Optical Imaging Center (BIOPIC), Peking-Tsinghua Center for Life Sciences, State Key Laboratory of Protein and Plant Gene Research, School of Life Sciences, Peking University, Beijing 100871, China; Tsinghua-Peking Joint Center for Life Sciences; State Key Laboratory of Bio-membrane and Membrane Biotechnology, School of Life Sciences and School of Medicine, Tsinghua University, Beijing 100084, China

Correspondence: wswei@pku.edu.cn (W.W.)

**Running title**: BECN1 is not required for LC3 lipidation
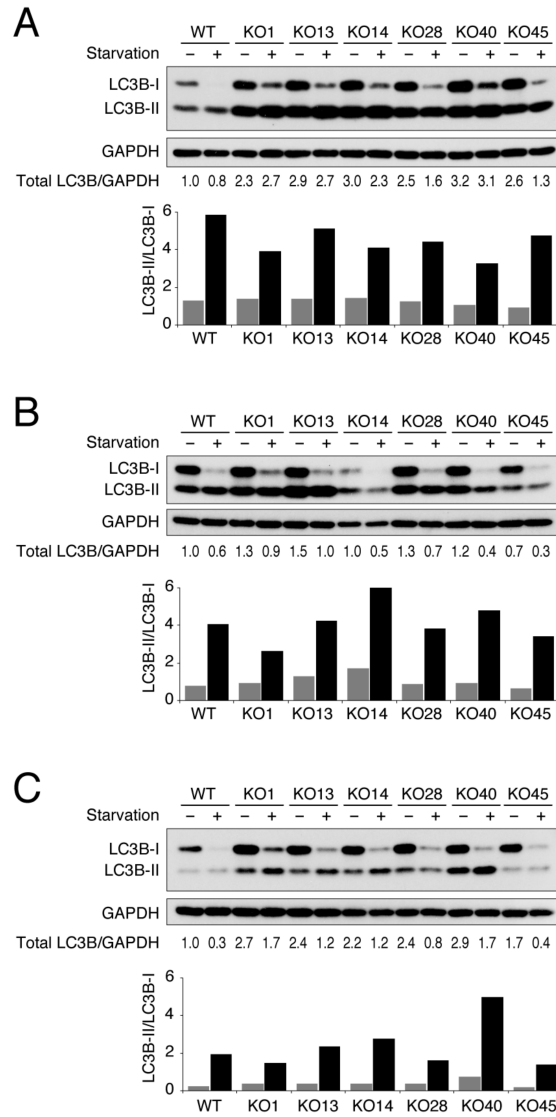
Figure S1. BECN1 is not required for LC3/LC3B lipidation during autophagy induction. (**A to C**) Three independent repeats of the immunoblotting analysis of the levels of LC3B-I and LC3B-II of the indicated cells treated with amino acid starvation for 4 h. The GAPDH bands were used as internal protein loading controls. The total LC3B/GAPDH is shown by numbers below each gel lane, and the quantification of relative levels of LC3B-II/LC3B-I is shown by bar graph.
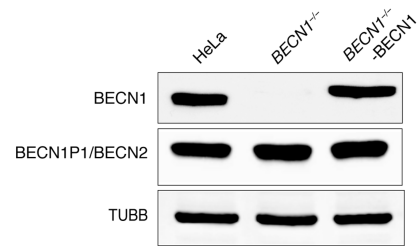
Figure S2. Immunoblotting analysis of BECN1P1/BECN2 in the indicated HeLa cells. The monoclonal antibodies targeting N-terminal BECN1 and BECN1P1 were used.
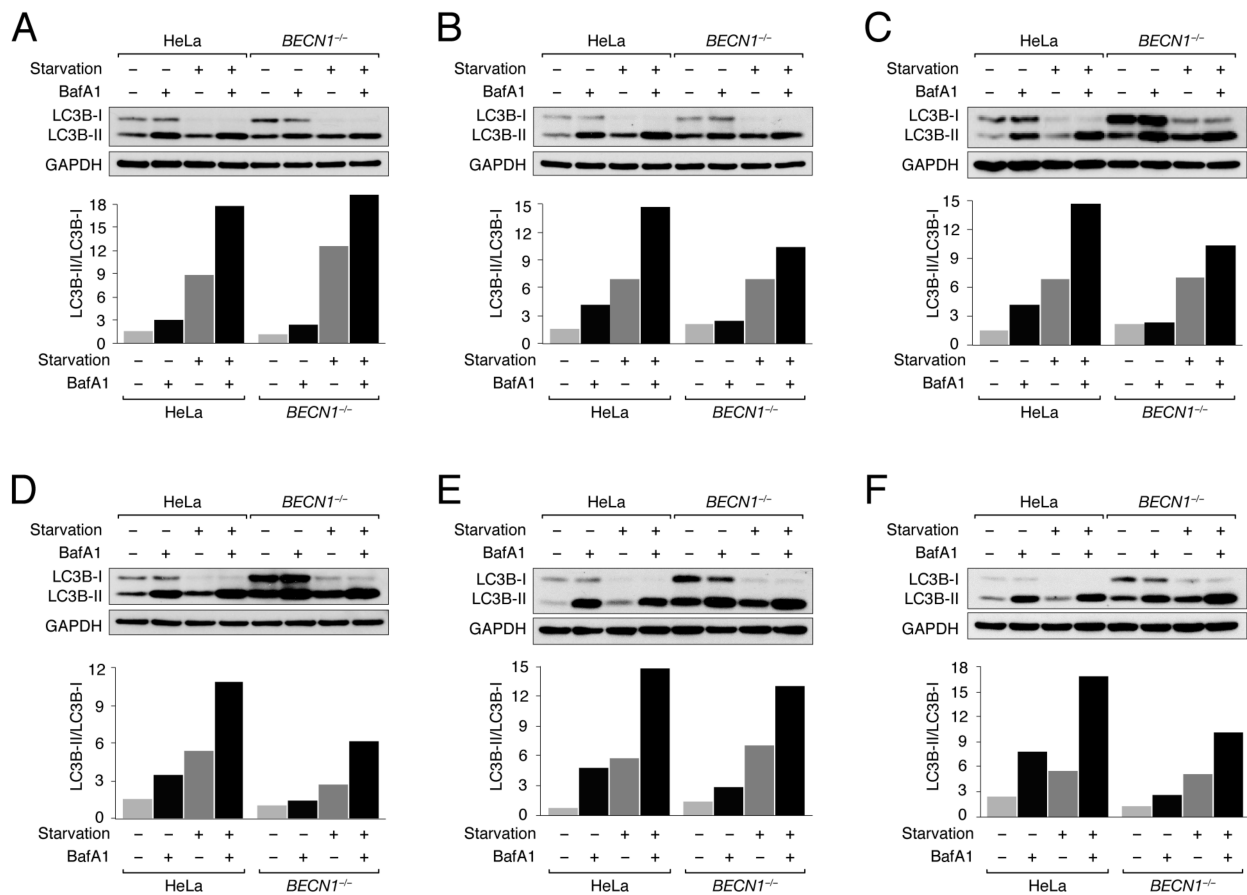
Figure S3. Effect of BECN1 on autophagy flux. (**A to F**) Six repeats for the immunoblotting analysis of LC3B turnover in the indicated HeLa cells treated with amino acid starvation for 4 h in the presence or absence of the autophagy inhibitor BafA1. The lower bar graph shows the quantification of LC3B-II/LC3B-I ratio of the upper immunoblotting results.
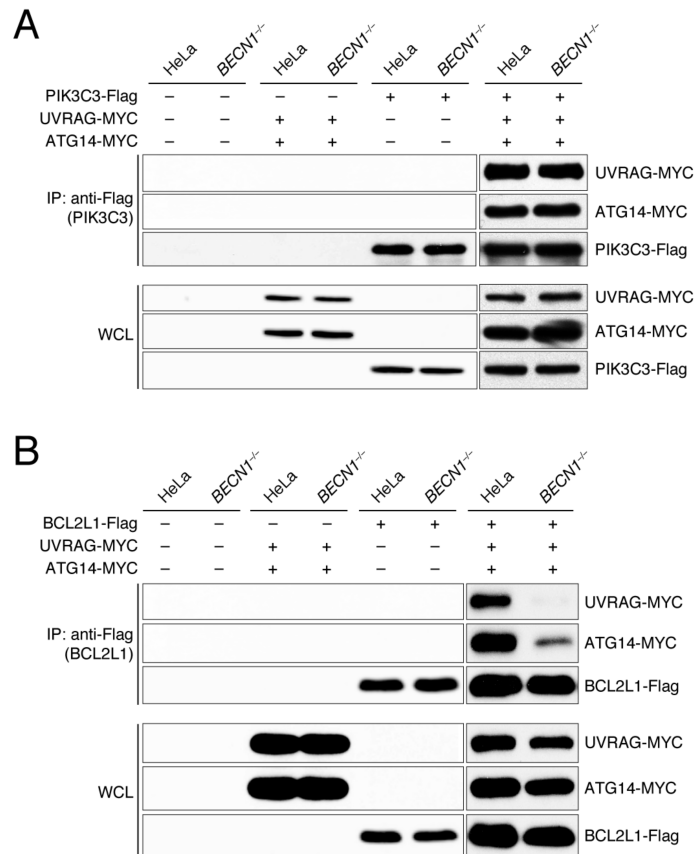
Figure S4. The role of BECN1 in PtdIns3K complex formation. (**A**) The protein-protein interaction between PIK3C3-Flag and ATG14-MYC or PIK3C3-Flag and UVRAG-MYC in the indicated HeLa cells. Cell lysates were immunoprecipitated with anti-Flag antibody for PIK3C3, compared to the whole cell lysate (WCL), and were immunoblotted using anti-MYC or anti-Flag monoclonal antibody as indicated. (**B**) The protein-protein interaction between BCL2L1-Flag and ATG14-MYC or BCL2L1-Flag and UVRAG-MYC in the indicated HeLa cells. Cell lysates were immunoprecipitated with anti-Flag antibody for BCL2L1 compared to WCL, and immunoblotted using anti-MYC or anti-Flag monoclonal antibody as indicated.